

Strong infrared spectral broadening in low-loss As-S chalcogenide suspended core microstructured optical fibers

M. El-Amraoui¹, J. Fatome¹, J. C. Jules¹, B. Kibler¹, G. Gadret¹, C. Fortier¹,
F. Smektala^{1,*}, I. Skripatchev², C.F. Polacchini², Y. Messaddeq², J. Troles³, L. Brilland⁴,
M. Szpulak⁵, G. Renversez⁶

¹ ICB Laboratoire Interdisciplinaire Carnot de Bourgogne, UMR 5209 CNRS-Université de Bourgogne, Av. A. Savary, 21078 Dijon, France.

² Institute of Chemistry – UNESP, P.O. Box 355, Araraquara, SP 14801-970, Brazil.

³ Sciences Chimiques de Rennes, UMR 6226 CNRS-Université de Rennes I, 35042 Rennes Cedex, France

⁴ PERFOS, 11, rue Louis de Broglie, 22300 Lannion, France

⁵ Institute of Physics, Wroclaw University of Technology, Wroclaw, Poland

⁶ Institut Fresnel, UMR CNRS 6133, Université d'Aix Marseille, 13397, Marseille, France

*frederic.smektala@u-bourgogne.fr

Abstract: We report the fabrication and characterization of the first guiding chalcogenide As₂S₃ microstructured optical fibers (MOFs) with a suspended core. At 1.55 μm, the measured losses are approximately 0.7 dB/m or 0.35 dB/m according to the MOF core size. The fibers have been designed to present a zero dispersion wavelength (ZDW) around 2 μm. By pumping the fibers at 1.55 μm, strong spectral broadenings are obtained in both 1.8 and 45-m-long fibers by using a picosecond fiber laser.

©2010 Optical Society of America

OCIS codes: (060.5295) Photonic crystal fibers; (190.4370) Nonlinear optics, fibers; (160.4330) Nonlinear optical materials; (160.2750) Glass and other amorphous materials; (060.2280) Fiber design and fabrication; (060.2270) Fiber characterization; (060.2390) Fiber optics, infrared

References and links

1. P. Kaiser, E. A. J. Marcatili, and S. E. Miller, "A New Optical Fiber," *Bell Syst. Tech. J.* **52**, 265–269 (1973).
2. G. P. Agrawal, *Application of nonlinear fiber optics*, Academic Press, Boston 2001.
3. P. St. J. Russell, "Photonic crystal fibers," *Science* **299**(5605), 358–362 (2003).
4. J. C. Knight, "Photonic crystal fibres," *Nature* **424**(6950), 847–851 (2003).
5. R. Rangelrojo, T. Kosa, E. Hajto, P. J. S. Ewen, A. E. Owen, A. K. Kar, and B. S. Weherrett, "Near-infrared optical non linearities in amorphous chalcogenides," *Opt. Commun.* **109**(1-2), 145–150 (1994).
6. F. Smektala, C. Quémard, L. LeNeindre, J. Lucas, A. Barthélémy, and C. De Angelis, "Chalcogenide glasses with large non-linear refractive indices," *J. Non-Cryst. Solids* **239**(1-3), 139–142 (1998).
7. F. Smektala, C. Quémard, V. Couderc, and A. Barthélémy, "Non linear optical properties of chalcogenide glasses measured by z-scan," *J. Non-Cryst. Solids* **274**(1-3), 232–237 (2000).
8. T. M. Monro, Y. D. West, D. W. Hewak, N. G. R. Broderick, and D. J. Richardson, "Chalcogenide holey fibres," *Electron. Lett.* **36**(24), 1998–2000 (2000).
9. F. Smektala, F. Désévéday, L. Brilland, P. Houzot, J. Troles, and N. Traynor, "Advances in the elaboration of chalcogenide photonic crystal fibers for the mid infrared," *SPIE* **6588**, 658803 (2007).
10. J. Troles, F. Smektala, G. Boudebs, A. Monteil, B. Bureau, and J. Lucas, "Chalcogenide glasses as solid state optical limiters at 1.064 μm," *Opt. Mater.* **25**(2), 231–237 (2004).
11. L. Brilland, F. Smektala, G. Renversez, T. Chartier, J. Troles, T. Nguyen, N. Traynor, and A. Monteville, "Fabrication of complex structures of Holey Fibers in chalcogenide glass," *Opt. Express* **14**(3), 1280–1285 (2006).
12. G. Vienne, A. Coillet, P. Grelu, M. El Amraoui, J. C. Jules, F. Smektala, and L. Tong, "Demonstration of a Reef Knot Microfiber Resonator," *Opt. Express* **17**(8), 6224–6229 (2009).
13. M. R. E. Lamont, B. Luther-Davies, D. Y. Choi, S. Madden, and B. J. Eggleton, "Supercontinuum generation in dispersion engineered highly nonlinear (gamma = 10 /W/m) As₂S₃ chalcogenide planar waveguide," *Opt. Express* **16**(19), 14938–14944 (2008).

14. L. B. Fu, M. Rochette, V. G. Ta'eed, D. J. Moss, and B. J. Eggleton, "Investigation of self-phase modulation based optical regeneration in single mode As₂Se₃ chalcogenide glass fiber," *Opt. Express* **13**(19), 7637–7644 (2005).
15. D. P. Wei, T. V. Galstian, I. V. Smolnikov, V. G. Plotnichenko, and A. Zohrabyan, "Spectral Broadening of femtosecond pulses in a single-mode As-S glass fiber," *Opt. Express* **13**(7), 2439–2443 (2005).
16. L. Fu, V. G. Ta'eed, E. C. Mägi, I. C. M. Littler, M. D. Pelusi, M. R. E. Lamont, A. Fuerbach, H. C. Nguyen, D. I. Yeom, and B. J. Eggleton, "Highly non linear chalcogenide fibers for all-optical signal processing," *Opt. Quantum Electron.* **39**(12–13), 1115–1131 (2007).
17. J. S. Sanghera, C. M. Florea, L. B. Shaw, P. Pureza, V. Q. Nguyen, M. Bashkansky, Z. Dutton, and I. D. Aggarwal, "Non linear properties of chalcogenide glasses and fibers," *J. Non-Cryst. Solids* **354**(2–9), 462–467 (2008).
18. M. Szpulak, and S. Février, "Chalcogenide As₂S₃ suspended core fiber for mid-IR wavelength conversion based on degenerate four-wave mixing," *IEEE Photon. Technol. Lett.* **21**(13), 884–886 (2009).
19. C. Chaidhari, T. Suzuki, and Y. Ohishi, "Design of zero chromatic dispersion chalcogenide As₂S₃ glass nanofibers," *J. Lightwave Technol.* **27**(12), 2095–2099 (2009).
20. G. Renversez, B. Kuhlmeiy, and R. McPhedran, "Dispersion management with microstructured optical fibers: ultraflattened chromatic dispersion with low losses," *Opt. Lett.* **28**(12), 989–991 (2003).
21. P. Domachuk, N. A. Wolchover, M. Cronin-Golomb, A. Wang, A. K. George, C. M. B. Cordeiro, J. C. Knight, and F. G. Omenetto, "Over 4000 nm bandwidth of mid-IR supercontinuum generation in sub-centimeter segments of highly nonlinear tellurite PCFs," *Opt. Express* **16**(10), 7161–7168 (2008).
22. M. Liao, C. Chaudhari, G. Qin, X. Yan, T. Suzuki, and Y. Ohishi, "Tellurite microstructure fibers with small hexagonal core for supercontinuum generation," *Opt. Express* **17**(14), 12174–12182 (2009).
23. G. Qin, X. Yan, C. Kito, M. Liao, C. Chaudhari, T. Suzuki, and Y. Ohishi, "Supercontinuum generation spanning over three octaves from UV to 3.85 μm in a fluoride fiber," *Opt. Lett.* **34**(13), 2015–2017 (2009).
24. C. Fortier, J. Fatome, S. Pitois, F. Smektala, G. Millot, J. Troles, F. Désévéday, P. Houizot, L. Brilland, and N. Traynor, "Experimental investigation of Brillouin and Raman scattering in a 2SG sulfide glass microstructured chalcogenide fiber," *Opt. Express* **16**(13), 9398–9404 (2008).
25. F. Désévéday, G. Renversez, J. Troles, L. Brilland, P. Houizot, Q. Coulombier, F. Smektala, N. Traynor, and J. L. Adam, "Te-As-Se glass microstructured optical fiber for the middle infrared," *Appl. Opt.* **48**(19), 3860–3865 (2009).
26. F. Désévéday, G. Renversez, L. Brilland, P. Houizot, J. Troles, Q. Coulombier, F. Smektala, N. Traynor, and J. L. Adam, "Small-core chalcogenide microstructured fibers for the infrared," *Appl. Opt.* **47**(32), 6014–6021 (2008).
27. G. Boudebs, F. Sanchez, J. Troles, and F. Smektala, "Non linear optical properties of chalcogenide glasses: comparison between Mach-Zehnder interferometry and Z-scan techniques," *Opt. Commun.* **199**(5–6), 425–433 (2001).
28. G. E. Snopatin, M. F. Churbanov, A. A. Pushkin, V. V. Gerasimenko, E. M. Dianov, and V. G. Plotnichenko, "High purity arsenic-sulfide glasses and fibers with minimum attenuation of 12 dB/km," *Optoelectron. Adv. Mater.-Rapid Commun.* **3**(7), 669–671 (2009).
29. F. Zolla, G. Renversez, A. Nicolet, B. Kuhlmeiy, S. Guenneau, and D. Felbacq, "Foundations of Photonic Crystal Fibres", *Imperial College Press*, London, ISBN: 1–86094–507–4, (2005).
30. M. Szpulak, W. Urbanczyk, E. Serebryannikov, A. Zheltikov, A. Hochman, Y. Leviatan, R. Kotynski, and K. Panajotov, "Comparison of different methods for rigorous modeling of photonic crystal fibers," *Opt. Express* **14**(12), 5699–5714 (2006).
31. J. M. Dudley, G. Genty, and S. Coen, "Supercontinuum generation in photonic crystal fiber," *Rev. Mod. Phys.* **78**(4), 1135–1184 (2006).
32. G. Renversez, F. Bordas, and B. T. Kuhlmeiy, "Second mode transition in microstructured optical fibers: determination of the critical geometrical parameter and study of the matrix refractive index and effects of cladding size," *Opt. Lett.* **30**(11), 1264–1266 (2005).
33. G. Barton, M. A. V. Eijkelenborg, G. Henry, C. J. Large, and J. Zagari, "Fabrication of microstructured polymer optical fibres," *Opt. Fiber Technol.* **10**(4), 325–335 (2004).
34. J. C. Knight, T. A. Birks, P. S. J. Russell, and D. M. Atkin, "All-silica single-mode optical fiber with photonic crystal cladding," *Opt. Lett.* **21**(19), 1547–1549 (1996) (REMOVED HYPERLINK FIELD) (REMOVED HYPERLINK FIELD).
35. M. F. Churbanov, I. V. Scripachev, G. E. Snopatin, V. S. Shiryaev, and V. G. Plotnichenko, "High purity glasses based on arsenic chalcogenides," *J. Optoelectron. Adv. Mater.* **3**, 341–349 (2001).
36. J. Fatome, C. Fortier, T. N. Nguyen, T. Chartier, F. Smektala, K. Messaad, B. Kibler, S. Pitois, G. Gadret, C. Finot, J. Troles, F. Désévéday, P. Houizot, G. Renversez, L. Brilland, and N. Traynor, "Linear and Nonlinear Characterizations of Chalcogenide Photonic Crystal Fibers," *J. Lightwave Technol.* **27**(11), 1707–1715 (2009).
37. W. Li, S. Seal, C. Rivero, C. Lopez, K. Richardson, A. Pope, A. Schulte, S. Myneni, H. Jain, K. Antoine, and A. C. Miller, "Role of S/Se ratio in chemical bonding of As–S–Se glasses investigated by Raman, X-ray photoelectron, and extended X-ray absorption fine structure spectroscopies," *J. Appl. Phys.* **98**(5), 053503 (2005).

38. R. Stegeman, G. Stegeman, P. Delfyett, Jr., L. Petit, N. Carlie, K. Richardson, and M. Couzi, "Raman gain measurements and photo-induced transmission effects of germanium- and arsenic-based chalcogenide glasses," *Opt. Express* **14**(24), 11702–11708 (2006).
39. M. Liao, C. Chaudhari, G. Qin, X. Yan, C. Kito, T. Suzuki, Y. Ohishi, M. Matsumoto, and T. Misumi, "Fabrication and characterization of a chalcogenide-tellurite composite microstructure fiber with high nonlinearity," *Opt. Express* **17**(24), 21608–21614 (2009).
40. H. Ebendorff-Heidepriem, P. Petropoulos, S. Asimakis, V. Finazzi, R. Moore, K. Frampton, F. Koizumi, D. Richardson, and T. Monro, "Bismuth glass holey fibers with high nonlinearity," *Opt. Express* **12**(21), 5082–5087 (2004).
41. C. Finot, B. Kibler, L. Provost, and S. Wabnitz, "Beneficial impact of wave-breaking for coherent continuum formation in normally dispersive nonlinear fibers," *J. Opt. Soc. Am. B* **25**(11), 1938–1948 (2008).
42. J. M. Dudley, G. Genty, and S. Coen, "Supercontinuum generation in photonic crystal fiber," *Rev. Mod. Phys.* **78**(4), 1135–1184 (2006).

1. Introduction

Since the seminal article written by Kaiser, Marcatili, and Miller in 1973 [1], microstructured optical fibers (MOFs) have attracted much attention to control modal properties including overall losses. More recently, nonlinear optics is used in many applications, see for example [2], most of them being based on silica fibers [3,4]. One way to generalize these applications is to extend upward the useful wavelengths to the middle infrared and to increase material nonlinearities. It is well known that chalcogenide glasses are promising candidates for such improvements, and thus they have an important potential for non linear optics [5–7]. During the last decade, a great attention has been paid to the development of chalcogenide glass waveguides, including microstructured optical fibres, for different applications such as light amplification, optical regeneration and supercontinuum generation [8–17]. In this context, the ability to elaborate efficient highly non linear single-mode chalcogenide optical fibres, with desired performance parameters, as well as the development of approaches to monitor these parameters are of great importance. More precisely, the design of microstructured optical fibers is a way to both increase the nonlinearity of the waveguide and control its losses and chromatic dispersion [18–20]. The latter parameter is a key tool to obtain an efficient light conversion and to reach accordable fibered broadband sources in the mid infrared. Much effort has been recently devoted to obtain MOF from various glasses [21–23]. Nevertheless, an efficient conversion up to 5 μm to cover entirely the 3-5 μm window is still a target to reach. Our choice is thus to use strongly non linear chalcogenide fibres, which transparency extends at least up to 5 μm . These glasses are up to now the best compromise between material infrared transparency and non linear coefficient [6,7], by comparison with other non oxide glasses, such as heavy oxide or fluoride glasses. However, the elaboration of low losses chalcogenide MOFs is still a challenging issue [11, 24–26]. Among the numerous chalcogenide glasses, we have chosen the arsenic trisulphide (As_2S_3) glass. Indeed, this glass shows high non linear properties. The non linear refractive index n_2 is measured between 3 and 5 $10^{-18} \text{ m}^2/\text{W}$ depending on the wavelength [13, 27]. This composition shows also a high drawing capability and potential very low losses [28].

In this work, we report the fabrication of the first low loss suspended core chalcogenide microstructured optical fiber, with chromatic dispersion management, together with the demonstration of a spectral broadening toward infrared wavelengths. The realization of these fibers has been reached thanks to a bilateral project Fapesp-CNRS, between ICB-Université de Bourgogne France and The Institute of Chemistry, Araraquara, Brazil.

The article is organized as follows: first we describe the fiber design we have realized to optimize the spectral broadband generation. Then, we present the fabrication process of the As_2S_3 glass and the fiber drawing. Finally, we show the experimental linear and nonlinear characterizations of our fibers. From comparison with numerical simulations, we are able to validate the experimental results. The presented work has important consequences for the application of future As_2S_3 MOF-based devices for wavelength conversion in the mid-infrared.

2. As₂S₃ suspended core fiber design for broadband generation

Our long-term objective is to get an As₂S₃ MOF to generate a supercontinuum covering the full 3-5 μm range. To reach it, one solution is to shift downward the zero dispersion wavelength (ZDW) of the MOF to a value below 2.2 μm in order to be able to pump the fiber in the anomalous dispersion regime using a source around 2.1 μm . Such a control of the chromatic dispersion can be obtained using two kinds of MOF profiles: the conventional one based on a subset of a triangular lattice of holes and the suspended core one. Nevertheless, the former design with its required tiny pitches needs too many rings of holes for the current chalcogenide MOF technology to get guiding losses below material ones [11,20,26]. Consequently, only the suspended core profile can be currently considered to reach our objective.

We compute the dispersion properties of several suspended core MOFs corresponding to cross-section profiles already obtained during preliminary drawings. These simulations are realized, from scanning electron microscope images, using the finite element method [29,30]. Due to the core shape (see section 4.1.2), the chromatic dispersion curves we obtain (Fig. 1) are slightly different from the results already published for the same glass [18]. As it can be seen, the waveguide chromatic dispersion D_w is able to compensate for the strongly negative material chromatic dispersion D_{mat} and make the overall dispersion D positive around 2 μm . Consequently, it is possible to design a suspended core MOF made of As₂S₃ glass with a realistic cross-section profile which has its anomalous regime starting around 2 μm . In our case for a 2.3 μm core size MOF profile the ZDW is at 2.12 μm whereas it is at 2.21 μm for a 2.6 μm core size configuration. These computed ZDW exhibit a strong shift towards shorter wavelengths compared to the ZDW of the As₂S₃ bulk approximately equal to 5 μm (Fig. 1). It is worth mentioning that the smaller the core size the steeper the chromatic dispersion D . Since it is known from previous work [31] that flattened dispersion near ZDW is more favourable to supercontinuum generation than D high slope configuration, we can deduce that a trade-off must be chosen between a smaller ZDW and a smaller D slope. Furthermore, as it can be seen in Fig. 1, the position of the ZDW strongly depends on the core size value. The next issue is the guiding losses. As already pointed out in reference [1], suspended core MOF can be either single mode or multimode according to fiber geometrical parameters. It is worth adding that the material refractive index also plays a crucial role [32]. For the smallest core size MOF profile, the fundamental mode guiding losses (losses computed without any material losses) are below 0.1 dB/m for λ below 5 μm and are smaller than $5.0 \cdot 10^{-5}$ dB/m for λ below 3 μm . This means that the material losses (of the 1 dB/m order of magnitude) will be the limiting factor, at least below 5 μm . Concerning the multimode behavior, the second mode losses are above $1.0 \cdot 10^{+3}$ dB/m for λ above 5 μm and above 70 dB/m for λ above 4 μm . They are under the 2 dB/m level below 3 μm . As a result, assuming no material losses, the single mode behavior of this suspended core MOF is limited to the upper part of the 3-5 μm window. For wavelengths smaller than 3 μm , the fiber cannot be considered as single mode. These results related to the fiber single modedness will be discussed in more details in section 4.1.4 when material losses are taken into account.

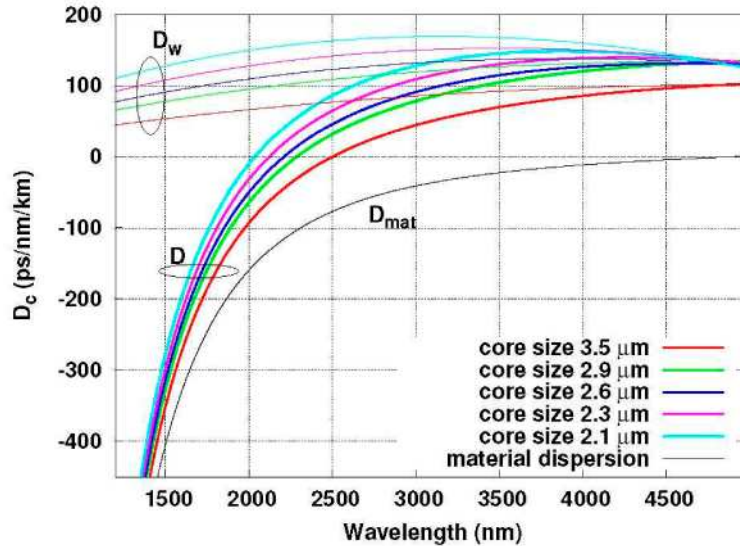


Fig. 1. : Computed waveguide chromatic dispersion D_w (thin upper curves), chromatic dispersion D (thick lower curves) for several suspended core As_2S_3 MOF. Material chromatic dispersion D_{mat} (black line). The configurations with a core size of 2.3 and 2.6 μm correspond to the two MOFs studied in section 4. The Sellmeier coefficients are the ones given for As_2S_3 by J. S. Browder & al. in Handbook of Infrared Optical Materials, P. Klocek editor, Marcel Dekker, ISBN: 0-8247-8468-5, (1991).

3. As_2S_3 glass and suspended core fibers fabrication

Arsenic trisulfide bulk glass (As_2S_3) is prepared by melting high purity (5N) elemental arsenic and sulfur in evacuated and vacuum sealed silica ampoules, placed in a rocking furnace at 700°C for 12 h. Some distillations are previously realized in order to purify starting elements from their remaining pollutants such as water or carbon. After refining, the silica ampoule containing the glass melt is quenched at room temperature. The solid glass rod obtained is then immediately annealed around glass transition temperature ($\approx 200^\circ C$) for 10h. A typical batch weight is 60g. The glass rod is typically 7 cm length for 16 mm diameter. There are several different techniques to elaborate preforms for microstructured fibers depending on the material (silica, non-silica, polymer etc). For soft materials, such as polymers for example, the holes can be directly drilled in the preform [33]. In the case of silica, the most convenient way is a handy preparation of the preform. The most used technique consists in staking capillaries and rods, thus forming on a macroscopic scale, the desired fiber microscopic geometry [34]. This procedure is usually called ‘stack-and-draw’ and is used when it is possible to obtain high optical and geometrical quality tubes that can be subsequently drawn to capillaries. Those are then stacked to form the desired preform, which is finally pulled to fiber. However, this technique presents many disadvantages concerning the optical qualities of MOFs, in particular for chalcogenide ones. It is time consuming due to multiples stages of the elaboration, there are surfaces degradation caused by handy manipulation, and the presence of interstitial holes. These features implicate higher optical losses. To overcome these problems and to avoid the multiple steps imposed by the stack and draw procedure, we have chosen an alternative technique. After annealing, the glass rod undergoes mechanical machining to get three holes of typically 1 mm diameter and 40 mm length around a solid core. The preforms prepared this way are then drawn into fibers.

4. Experimental and numerical results

4.1 Linear optical characterizations

4.1.1 Optical losses of As_2S_3 single index fibers

Initially we have measured the losses of single index fibers obtained by the drawing of As_2S_3 glass rods, in order to check the level of losses of the initial bulk glass, before any machining of the preform. The measurements are realized by the cut back technique with the help of a FTIR spectrophotometer, between 2 and 6 μm . Figure 2 presents the typical attenuation curve of these fibers. The results illustrate the good optical quality of the bulks reached in our glass elaboration process.

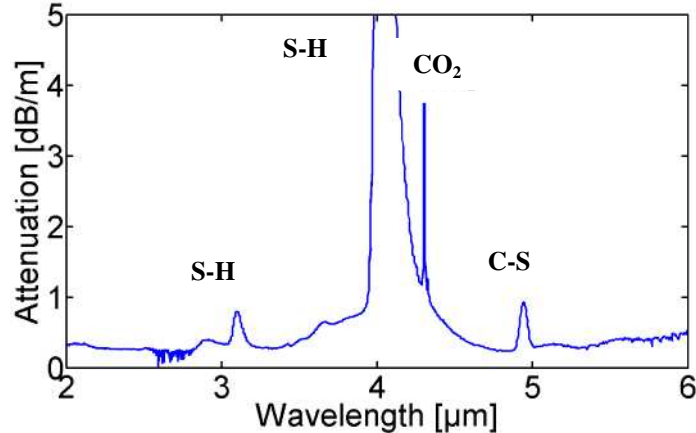


Fig. 2. Typical attenuation curve of a single index As_2S_3 optical fiber.

The background level of losses is around 0.4 dB/m between 2 and 6 μm . We observe an extrinsic S-H absorption band at 4 μm . This absorption (22 dB/m) corresponds to a residual SH pollution of the glass. The extinction coefficient associated to the SH vibration being 2.5 dB/m/ppm [35] at 4 μm , the residual SH content is of only 9 ppm.

4.1.2 Geometrical profiles of As_2S_3 suspended core fibers

We have observed the sections of the fibers obtained by the drawing of machined preforms by scanning electron microscopy (SEM). In Fig. 3 are presented the SEM pictures of the two fibers that are under study in this work. Suspended core fibers presenting three holes around a solid core in a triangular shape have effectively been obtained, with a very good control of the geometry. From these images, we have measured the core diameter of the fibers, defined as the diameter of the circle inscribed in the triangular core. Typically two different core sizes have been obtained, 2.6 μm and 2.3 μm . These values are really close to the diameter predicted from numerical simulations in order to reach a zero dispersion wavelength (ZDW) close to 2.1 μm .

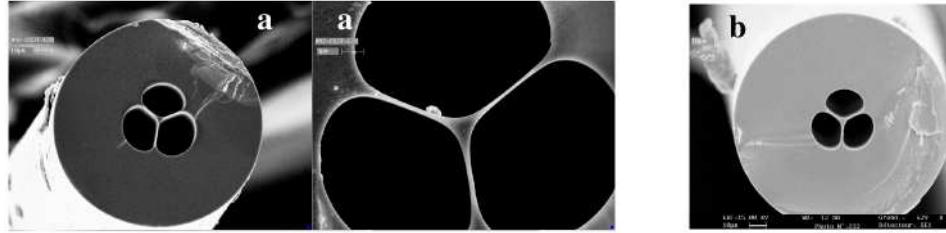


Fig. 3. SEM pictures of two As_2S_3 suspended core fibers with a core size of $2.6\mu\text{m}$ (a) and $2.3\mu\text{m}$ (b).

4.1.3 Optical losses of As_2S_3 suspended core fibers

We have then measured the losses of the suspended core MOFs. Due to the small core of these fibers, it was not possible to obtain the spectral attenuation curve using our FTIR spectrophotometer. We have then realized discrete measurements with the help of a fibered source at $1.55\mu\text{m}$. On 2 meters of the $2.6\text{-}\mu\text{m}$ core MOF, the losses are found to be 0.7 dB/m . On 45 meters of the $2.3\text{-}\mu\text{m}$ core MOF, the losses are found to be 0.35 dB/m . These values are fully consistent with the attenuations obtained on single index fibers (see Fig. 2), and illustrate the very good quality of our chalcogenide MOFs. What's more, the machining process we have developed allow to obtain microstructured fibers without any excess of losses due to the preform elaboration process, as it is generally observed with the stack and draw procedure. Thus, the losses level we have obtained is ten times lower than the best one reported for chalcogenide MOF fabricated by the stack and draw technique [24] and corresponds to the best of our knowledge to the lowest optical losses reported to date on chalcogenide MOFs.

From these loss measurements and the results given in section 2, it can be deduced that, for the fundamental mode, the limiting factor are the material losses and not the guiding ones. The preliminary results already given can be completed taking into account the material losses. The overall losses can be computed adding a global positive imaginary part at the relative electric permittivity of the matrix. It will be named ϵ_{imag} and it depends on the wavelength. Since the average material loss level is 0.4 dB/m in the range $2\text{-}6\mu\text{m}$ (except around the SH peak), we get $\epsilon_{\text{imag}}=5.54\cdot 10^{-6}$ at $1.55\mu\text{m}$ (assuming that the material losses at $1.55\mu\text{m}$ are equal to the average loss level), $\epsilon_{\text{imag}}=1.07\cdot 10^{-6}$ at $3\mu\text{m}$, and $\epsilon_{\text{imag}}=1.79\cdot 10^{-6}$ at $5\mu\text{m}$. For the $2.3\mu\text{m}$ core size MOF profile and the three considered wavelengths, the fundamental mode losses are around 0.4 dB/m whereas the second mode ones are now similar to the fundamental mode one (around 0.4 dB/m up to $2\mu\text{m}$) but around 2 dB/m at $3\mu\text{m}$, and above 70 dB/m for λ above $4\mu\text{m}$. Consequently, we can confirm that, taking into account the material losses, the MOF cannot be considered as single mode in the short wavelength window of the infrared atmospheric transmission band but it remains single mode, as stated in section 2, in its upper part due to the differential guiding loss between the fundamental and the second modes. The remaining issue is that the pump wavelength fixed either around $1.55\mu\text{m}$ or around $2\mu\text{m}$ will be in the multimode regime of the suspended core MOF. While these characteristics may have some negative influence on the supercontinuum generation, reasonable broadening is still expected, as demonstrated in probably multimode tellurite suspended core MOF already [21].

4.1.4 Suspended core MOF dispersion properties

We have measured the chromatic dispersion of our suspended core fiber (core diameter $2.3\mu\text{m}$ and $2.6\mu\text{m}$) around $1.55\mu\text{m}$, on 50 cm fiber length (Fig. 4).

The measurement setup is based on the well-known interferometric method, which is particularly suitable to characterize short segments of optical fiber [36]. The home-made interferometric setup consists of an all-fiber Mach-Zehnder interferometer, in which the reference arm was made of an integrated fiber delay-line spliced to two broadband $50:50$

couplers. The chalcogenide MOF under-test was inserted into the test path by means of two fiber splicers and micro-lens fibers in order to minimize injection losses. The resulting interference pattern was monitored in the frequency domain thanks to an optical spectrum analyzer (OSA) and the chromatic dispersion was deduced from the evolution of the central fringe wavelength with respect to the reference arm delay [36]. Experimental results (circles and triangles) are plotted in Fig. 4 and compared with numerical simulations for both chalcogenide MOFs.

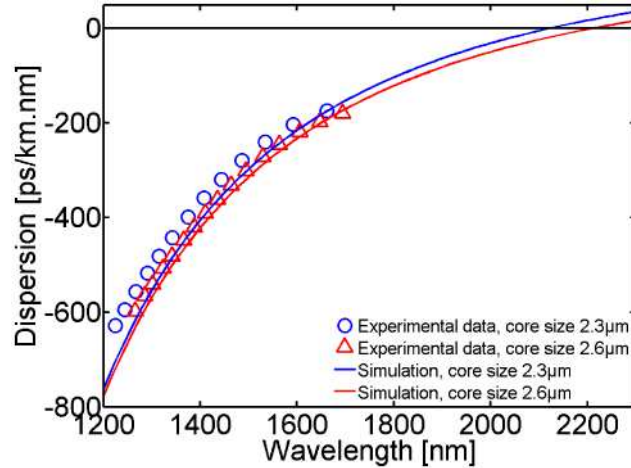


Fig. 4. : Comparison between the experimental chromatic dispersion curves of 2.3- μm (circles) and 2.6- μm (triangles) As_2S_3 suspended core fibers and their corresponding numerical results (blue and red solid lines, respectively).

The experimental chromatic dispersion was found to be $D = -240$ and -280 ps/nm.km around 1550 nm for the 2.3- μm and 2.6- μm core MOFs respectively, with dispersion slope about 1 ps/nm².km. One can notice the good agreement between experimental and theoretical values. Since the computed ZDW are around 2.1 μm and 2.2 μm for the 2.3 μm and the 2.6 μm core MOFs respectively, we can expect that the experimental ZDW of the two fibers are close to the targeted value of 2.1 μm .

4.2 Non linear optical characterizations

4.2.1 Self-phase modulation and Raman scattering

The nonlinear features of our suspended core chalcogenide fibers were first characterized in a 1.8-m long sample (2.6 μm of core diameter and 0.7 dB/m losses). An amplified PRITEL mode-locked fiber laser generating 8-ps pulses at a repetition rate of 22 MHz around 1550 nm was injected into the PCF. The injection test-bed consists of a 2.7- μm mode filed diameter micro-lens fiber aligned with a splicing machine, which allow us to achieve 4-dB insertion losses. The input average power is controlled by a variable attenuator coupled with an inline power-meter. Note that a polarization controller is also placed just before injection in order to maximize the self-phase modulation (SPM) induced spectral broadening within the chalcogenide fiber. At the output of the fiber, the signal is finally monitored thanks to an optical spectrum analyzer (OSA).

Figure 5 shows the experimental results (blue lines) obtained for increasing input powers. We can observe in Fig. 5a that pulses undergo typical self-phase modulation behaviour with induced spectral broadening and oscillations appearance. On the other hand, as illustrated in Fig. 5 (b, c) on a wide range of wavelengths, we note the generation of a spontaneous Raman scattering stokes wave centred on 1635 nm, which confirms the strong Raman gain and the 10.1-THz (85-nm) Raman shift exhibit by MOF chalcogenide fibers [24].

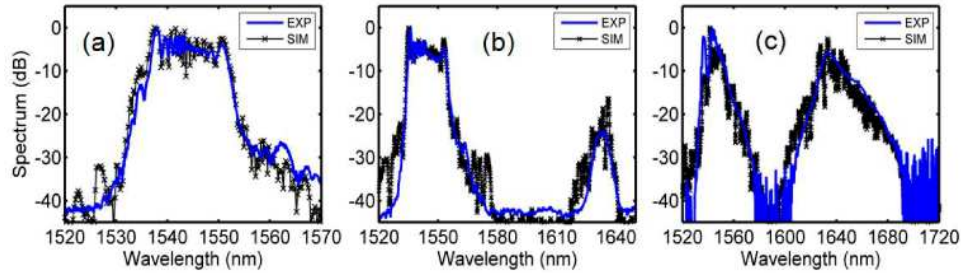


Fig. 5. : Output spectra (blue solid line) recorded from the 1.8-m long 2.6- μm core diameter suspended core fiber for input peak powers of (a) 18 W (b) 28 W and (c) 54 W. Corresponding numerical simulations are also reported with black lines and crosses.

In order to determine the nonlinear Kerr coefficient of the 2.6 μm core chalcogenide fiber, we have performed numerical simulations based on the well-known split-step Fourier resolution of the generalized nonlinear Schrödinger equation [31]. The model takes into account the experimental chromatic dispersion and losses. It also includes Kerr, nonlinear (two-photon) absorption, self-steepening and Raman terms based on the previous studies of As_2S_3 glass [13, 24, 37, 38]. Numerical predictions (black lines and crosses) are compared to experimental spectra in Fig. 5 and show a pretty good agreement. Finally, from these calculations, we have deduced a nonlinear Kerr coefficient of $\gamma = 2150 \text{ W}^{-1}.\text{km}^{-1}$ which is 1600 times larger than a standard fused silica fiber G652.

4.2.2 Broadband spectrum generation

The pumping of our fibers in the anomalous regime, around 2.1 μm , is currently in progress. However, in order to demonstrate the nonlinear potential of our MOFs, we have injected the previous 8-ps 22-Mz mode-locked laser around 1.55 μm in the 45-m long sample of the 2.3- μm core MOF. Due to the 0.35 dB/m linear losses, the effective length of the configuration is 12 m, thus all the nonlinear effects take place in these first ten meters of the fiber. From numerical modal simulations we have calculated $\gamma = 2750 \text{ W}^{-1}.\text{km}^{-1}$. The figure of merit, defined as the product of the nonlinear coefficient and effective length was found to be 33 W^{-1} , one of the highest ever reported [39-40]. Figure 6 shows the experimental spectrum obtained at the output of the 45-m long MOF for the highest input peak power injected (54 W). Note that the input polarization state was adjusted so as to optimize the generation of the broadest spectrum. As illustrated in Fig. 6, we observe a strong spectral broadening. Its dynamics is mainly governed and limited by the normal dispersion regime induced wave breaking and is hopefully helped by Raman scattering [41-42]. Despite the fact that the observation is limited to 1700 nm due to the OSA wavelength range, we note that the long-wavelength edge of the spectrum probably reaches 1750 nm, resulting in more than 200-nm (at -20 dB) spanning continuum.

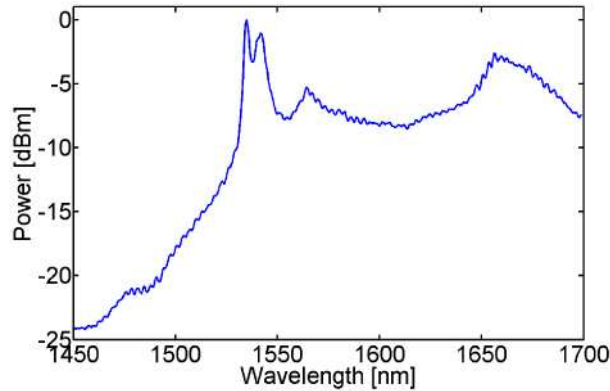


Fig. 6. : Spectrum recorded experimentally at the output of the 45-m long segment of our 2.3- μm suspended core fiber for an input peak power of 54 W.

5. Conclusion

We report, to the best of our knowledge, the first guiding chalcogenide suspended core microstructured optical fibers. The fiber design has been chosen to manage chromatic dispersion and losses. We note a very good agreement between the chromatic dispersion simulations and the corresponding measurements for 2.3 and 2.6 μm core size fibers. The fiber losses are measured to be as low as 0.35 dB/m at 1.55 μm for a 45 meters long 2.3 μm core size fiber. The related nonlinear Kerr coefficient is estimated as high as 2750 $\text{W}^{-1} \text{km}^{-1}$. By pumping the 2.3 μm core size fiber close to 1.55 μm with the help of a picosecond fiber laser, more than 200 nm spanning continuum is obtained in the infrared. These results are clearly of interest in the applicability of this novel class of highly nonlinear chalcogenide MOFs for future efficient light conversion experiments in the mid-infrared.

Acknowledgements

We would like to acknowledge the Conseil Regional de Bourgogne, the French DGA (contract 05.34.053), the bilateral French Brazilian CNRS Fapesp program, the Mission des Ressources et Compétences Technologiques du CNRS (project Chalcoapir), the Agence Nationale de la Recherche (FUTUR project 2006 TCOM 016) and the European COST Action 299.